2D Nanomaterials

DOI: 10.1002/anie.201309474

Patternable Large-Scale Molybdenium Disulfide Atomic Layers Grown by Gold-Assisted Chemical Vapor Deposition**

*Intek Song, Chibeom Park, Misun Hong, Jaeyoon Baik, Hyun-Joon Shin, and Hee Cheul Choi**

Abstract: *A novel way to grow MoS_2 on a large scale with uniformity and in desired patterns is developed. We use Au film as a catalyst on which $[Mo(CO)_6]$ vapor decomposes to form a Mo-Au surface alloy that is an ideal Mo reservoir for the growth of atomic layers of MoS_2. Upon exposure to H_2S, this surface alloy transforms into a few layers of MoS_2, which can be isolated and transferred on an arbitrary substrate. By simply patterning Au catalyst film by conventional lithographic techniques, MoS_2 atomic layers in desired patterns can be fabricated.*

Two-dimensional (2D) MoS_2 has gained much attention for its intrinsically semiconducting property that is absent in graphene.[1–5] To fully exploit such an advantage in various applications, it is required to secure uniform, large-scale, and patterned atomic layers of MoS_2. The patternability of MoS_2 is of special interest for the fabrication of MoS_2 atomic layers into complex hybrid heterostructures composed with different kinds of 2D nanomaterials.[6,7] As a consequence, there has been a rapid increase in the number of reports regarding large-scale synthesis of MoS_2 by chemical vapor deposition (CVD).[8–12] However, none of these syntheses has accomplished all of the properties of uniformity, scalability, and patternability owing to their intrinsic limitations.[13] Among these, the preparation of an atom-thick and uniform Mo layer over a wide area of a substrate, that is, a large-scale Mo reservoir, is currently the most difficult hurdle to overcome.

Herein, we report a novel way to prepare transferable few-layer MoS_2 structures in desired sizes and patterns with high uniformity by a gold catalyst-assisted CVD process. Our finding encompasses the following: 1) The Mo-Au surface alloy is readily formed by the low-temperature reaction of $[Mo(CO)_6]$ and pre-deposited Au thin film, which acts as a large-scale Mo reservoir; 2) large-scale MoS_2 atomic layers are successfully grown upon the subsequent reaction of the Mo-Au surface alloy with H_2S; 3) the resulting MoS_2 atomic layers are easily isolated from the substrate by etching Au layers; and 4) atomic layers of MoS_2 can be grown in specific patterns by simply defining the pattern of Au thin film.

Scheme 1 shows a flow chart to acquire large-scale and patterned MoS_2 atomic layers through the formation of a uniform Mo precursor reservoir by a Mo-Au alloy on a Au thin film. The formation of Mo-Au alloy, the key step to acquire a uniform and patternable Mo reservoir, is predicted from their phase diagram (Supporting Information, Figure S1).[14] For this, the Au film pre-deposited on a Si substrate was reacted with 0.1 atm of $[Mo(CO)_6]$ vapor followed by the reaction with H_2S at 300 °C under atmospheric pressure for sulfidation (Supporting Information, Figure S2a).[15] The sample shows no significant change of color (Figure 1 a).

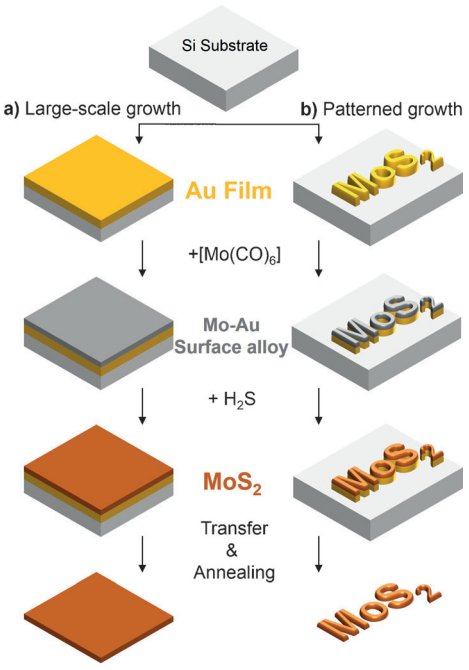

Scheme 1. CVD treatment of $[Mo(CO)_6]$ on Au thin film forms a Mo-Au surface alloy, which further reacts with H_2S to form MoS_2 atomic layers in large scale (a) and in a specific pattern (b). The as-grown MoS_2 atomic layers are easily removed from the Mo-Au alloy substrate and transferred to arbitrary substrates.

[*] I. Song, C. Park, M. Hong, H. C. Choi
Center for Artificial Low Dimensional Electronic Systems
Institute for Basic Science (IBS)
77 Cheongam-Ro, Nam-Gu, Pohang, 790-784 (Korea)
I. Song, C. Park, M. Hong, H. C. Choi
Department of Chemistry
Pohang University of Science and Technology (POSTECH)
77 Cheongam-Ro, Nam-Gu, Pohang, 790-784 (Korea)
E-mail: choihc@postech.edu
Homepage: http://www.postech.ac.kr/chem/nmrl
J. Baik, H.-J. Shin
Pohang Accelerator Laboratory and Department of Physics
Pohang University of Science and Technology (POSTECH)
77 Cheongam-Ro, Nam-Gu, Pohang, 790-784 (Korea)

[**] This work was partially supported by the National Research Foundation of Korea (NRF) grant (2010-00285, 2012R1A2A1A01003040, and 2009-0094036). I. Song is grateful to Global Ph.D. Fellowship grant from NRF (2012H1A2A1016525). We thank Pohang Accelerator Laboratory (Beamline 8A1).

Supporting information for this article is available on the WWW under http://dx.doi.org/10.1002/anie.201309474.

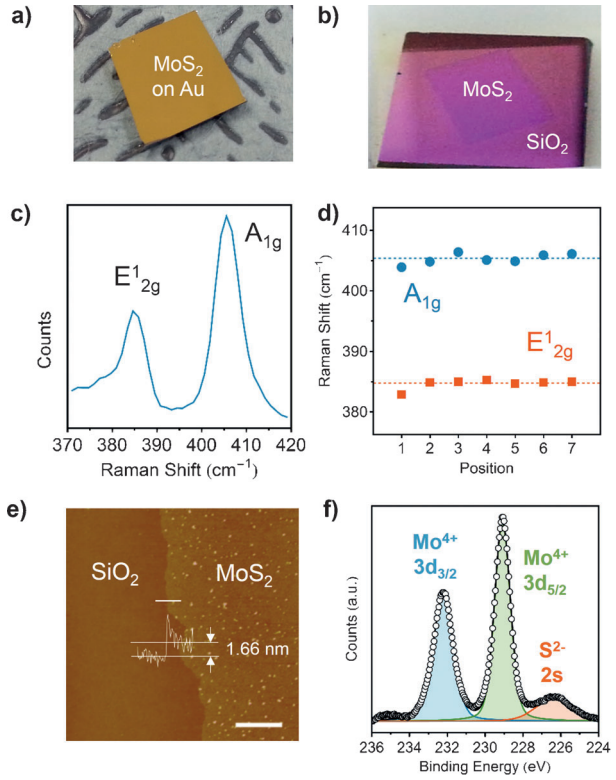

Figure 1. a), b) Optical images of as-grown MoS_2 atomic layers grown on Au film (a) and those transferred on a fresh SiO_2 (b). c) Representative Raman spectrum of MoS_2 atomic layers. d) Positions of Raman peaks measured at seven random positions. The dashed lines denote the mean values (A_{1g}: 405.4 cm^{-1}, E^1_g: 384.8 cm^{-1}). e) AFM image taken at the edge of transferred MoS_2 atomic layers. The scale bar denotes 10 μm. f) XPS data showing Mo^{4+} and S^{2-} in the Mo 3d and S 2s regions.

Note that high-quality MoS_2 atomic layers are occasionally obtained at this stage (Supporting Information, Figure S3). The sample was then etched with Au etchant and transferred to a SiO_2 substrate (Supporting Information, Figure S2b). Further reaction with H_2S at 800 °C enhances crystallinity and completes sulfidation (Supporting Information, Figure S2c).

A representative bright-field optical image of a final piece of MoS_2 atomic layers (2×2 cm^2) transferred on a SiO_2/Si substrate is shown in Figure 1b. The size and shape of the transferred MoS_2 layers are very well matched with those of Au film. The homogeneous color contrast induced by MoS_2 layers on a SiO_2/Si substrate implies that the as-grown MoS_2 is fairly uniform in thickness.

The successful formation of MoS_2 in atomic layers was initially characterized by Raman spectroscopy. A representative Raman spectrum of MoS_2 shows two characteristic peaks of E^1_{2g} and A_{1g} at 385.3 and 405.6 cm^{-1}, respectively (Figure 1c). The Raman spectra taken at seven different locations inside the sample (Figure 1d) and at the edge of the sample (Supporting Information, Figure S4) show comparable peak positions. This result supports the notion that the product is uniform over the large area. Furthermore, the energy difference of 20.3 cm^{-1} between E^1_{2g} and A_{1g} peaks suggest that the number of MoS_2 layers is two.[16] This inference is well supported by AFM results (Figure 1e) showing that the height of MoS_2 layers placed on a SiO_2/Si substrate is 1.6 nm, which matches to the height of two to three layers of MoS_2.

X-ray photoelectron spectroscopy (XPS) studies confirmed the chemical identity of MoS_2. The high-resolution spectrum of Mo 3d shows that there are two strong peaks at 232.6 eV ($3d_{3/2}$, blue) and 229.5 eV ($3d_{5/2}$, green) with one weak peak at 226.5 eV (S 2s, orange), all of which are deconvoluted into single Gaussian–Lorentzian curves (Figure 1f). The absence of peaks near 236 eV rules out the presence of Mo^{6+} and thus that of MoS_3. The S 2p spectrum clarifies that the oxidation state of S is −2 (Supporting Information, inset in Figure S5). Note that the presence of oxides is ruled out, as the O 1s spectrum only shows the presence SiO_2, not metal oxide peaks.

The quality and the number of layers of MoS_2 were further investigated by high-resolution transmission electron microscopy (HRTEM) using a sample transferred on a copper grid coated with amorphous carbon film. A typical HRTEM image of MoS_2 atomic layers shows distinct hexagonal atomic arrangements (Figure 2a), and its reciprocal space image obtained by its Fourier transform reveals clear hexagonal sets of dots (Figure 2b), matching with $P6_3/mmc$ of the crystallographic space group of MoS_2. The inner hexagon with the radius of 3.8 nm^{-1} corresponds to (100) planes with interplanar distance of 2.7 Å, and the outer with the radius of 6.3 nm^{-1} corresponds to (110) planes having interplanar distance of 1.6 Å in real space. These results imply that the zone axis is [001] direction, showing that the sample is indeed composed of a 2D atomic sheet lying on a substrate. The absence of hexagonal dots in different orientations indicates that the sample is single-crystalline at least within the range of scope, the diameter of which is several tens of nanometers. A noise-filtered HRTEM image obtained by selecting the hexagonal dots from Figure 2b clearly shows an ordered hexagonal symmetry of dots (Figure 2d), matching with a typical crystal structure of MoS_2 (Figure 2c) as well as with other reports.[17–19] Figure 2e is an HRTEM image taken at the region where MoS_2 atomic layers are folded, which provides an evidence for the formation of two to three MoS_2 atomic

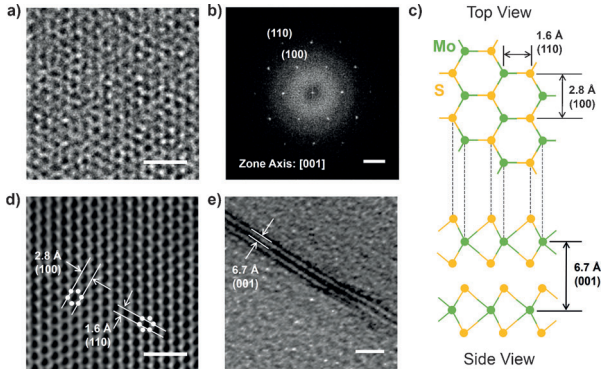

Figure 2. a) HRTEM image of MoS_2 showing hexagonal symmetry of the exiting wave function. The scale bar is 1 nm. b) Fourier-transformed electron diffraction of (a). The scale bar is 2 nm^{-1}. c) A ball-and-stick model of MoS_2 showing top and side views of the atomic structure. d) Fourier-filtered image of (a). The scale bar is 1 nm. e) Cross-section image of MoS_2 atomic layers exhibiting 6.7 Å interlayer distance. The scale bar is 2 nm.

layers. The inter-layer distance of 6.7 Å agrees well with the aforementioned value measured from the AFM image.

The electrical properties of MoS_2 atomic layers were investigated using MoS_2 field-effect transistor (FET) devices exhibiting the mobility of 0.004 $cm^2V^{-1}s^{-1}$. Details of the fabrication method and discussion are included in the Supporting Information (Figure S6).

Considering the fact that the same CVD reactions attempted on a bare SiO_2 or Si substrate without Au catalyst yields irregular MoS_2 particulates by both sequential (Supporting Information, Figure S7) and simultaneous injections of Mo and S precursors,[20,21] the formation of uniform and large-scale MoS_2 atomic layers by our method seems mainly attributed to the realization of large-scale and homogeneous Mo-Au alloy on the target substrate. This result, however, contradicts the bulk Mo-Au binary phase diagram (Supporting Information, Figure S1). The diagram states that the solubility of Mo in crystalline Au *fcc* structure is only up to 0.34 atomic % at 300 °C to form a homogenous substitutional alloy, and excess Mo should form separate crystalline Mo *bcc* islands. Our alloy system, in contrast, seems completely miscible, as the resulting MoS_2 is uniform in large area. This anomaly can be explained by the concept of a surface alloy. The surface alloy denotes an alloy that is confined to atom-thick layers at the surface, especially composed of a pair of elements that are immiscible in the bulk.[22] Therefore, the formation of surface alloy is often observed in various immiscible binary systems, such as K-Al[23] or Au-Ni,[24] where the atomic radius differs from each other significantly. One of the main driving forces to produce surface alloys of immiscible elements is the reduction of interface energy arising from the mismatch at near the surface. As a result, alloying occurs only at the surface at atomic thickness level.[22,24]

The successful formation of Mo-Au surface alloy was investigated by XPS (Figure 3a) and AFM (Supporting Information, Figure S8). When the Au surface is only reacted with $[Mo(CO)_6]$ vapor, its XPS spectrum shows two Mo 3d peaks appearing at 235.2 eV ($3d_{3/2}$) and 232.1 eV ($3d_{5/2}$). These Mo 3d binding energies are blue-shifted with respect to metallic Mo ($3d_{3/2}$: 228 eV, $3d_{5/2}$: 225 eV), which owes not to the oxide formation (Supporting Information, Figure S9) but to the charge transfer between Mo and Au atoms upon the formation of Mo-Au alloy at 300 °C.[25–27] Such shift of XPS peak is often observed in many alloy systems such as Ag-Au[28] or Pd-Au.[29] Their positions are also clearly differentiated from those of MoS_2 atomic layers. The XPS spectrum after sulfidation (Figure 3b) reveals successful formation of MoS_2, as three related peaks appearing at 232.5 eV (Mo^{4+} $3d_{3/2}$, blue), 229.4 eV (Mo^{4+} $3d_{5/2}$, blue), and 226.0 eV (S^{2-} 2s, orange). The other two green peaks have the same position as Mo-Au alloy, indicating that a certain portion of the alloy remains unreacted. This process does not involve the formation of other chemical species (Supporting Information, Figure S10). The uniformity of the Mo-Au surface alloy is confirmed by observing comparable XPS peak positions from five different locations of the sample.

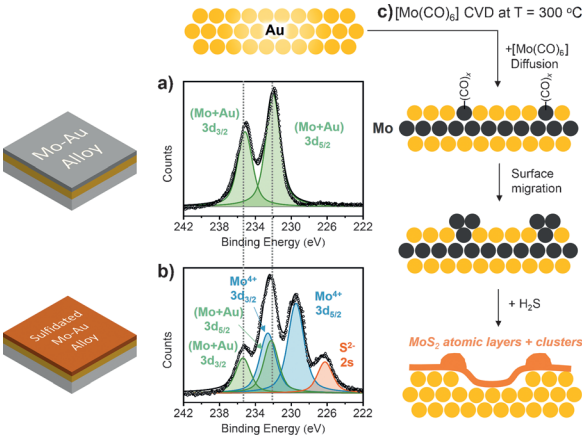

Figure 3. a), b) X-ray photoelectron spectrum at Mo 3d and S 2s regions for Mo-Au alloy (a) and sulfidated Mo-Au alloy (b). c) Proposed mechanism for the formation of Mo-Au surface alloy and atomic layers of MoS_2 at 300 °C. Incomplete dissociation of CO from $[Mo(CO)_6]$ results in Mo clusters that eventually yield MoS_2 clusters.

A notable surface feature of Mo-Au surface alloy is that the Mo layer goes underneath the topmost Au layer when pure Mo reacts with Au to minimize surface energy, while incompletely defragmentized Mo, such as $[Mo(CO)_x]$ ($0 < x < 6$), induces local aggregations through surface migration (Figure 3c; Supporting Information, Scheme S1).[27,30,31] The formation of such Mo clusters on Mo-Au surface alloy is confirmed by AFM (Supporting Information, Figure S8c).[25] When the Mo-Au surface alloy reacts with H_2S, the buried Mo layer is diffused out and sulfidated to form film-type MoS_2 layers as a major product while MoS_2 particles are formed from Mo clusters as a minor product (Supporting Information, Figure S8d).[30,32–34] The co-presence of both MoS_2 layer and particles is also found in Figure 1e. More detailed discussion about the reaction mechanism is available in the Supporting Information.

The critical role of Au as a support for the homogenous Mo precursor over a large area of substrate suggests that a patterned growth of MoS_2 atomic layers is feasible simply by defining the pattern of Au film. Thus, the direct formation of patterned MoS_2 atomic layers was attempted by running the CVD process using a Si substrate on which Au thin film was pre-patterned. Figure 4a and b show optical microscope images of pre-patterned Au thin film with letters of "MoS_2" and "M", respectively, having 1 μm of width of the line of each letter. After running CVD process at the same reaction condition used to obtain the samples shown in Figure 1 and 2, the patterned MoS_2 atomic layers were grown and transferred on a fresh SiO_2/Si substrate. As shown in Figure 4c and d, the shape and size of the transferred MoS_2 patterned atomic layers are well-retained. This is the first time to demonstrate the synthesis of few-layer MoS_2 in a desired pattern without any post-synthesis tailoring, of which resolution reaches down to sub-micrometers.

In summary, we have presented a novel way to synthesize MoS_2 atomic layers in desired sizes and patterns by Au-assisted CVD process. The successful growth of MoS_2 atomic layers in large-scale and patterned shape has been realized through securing Mo-Au surface alloy as a homogeneous and large-scale Mo precursor reservoir. The successive reaction

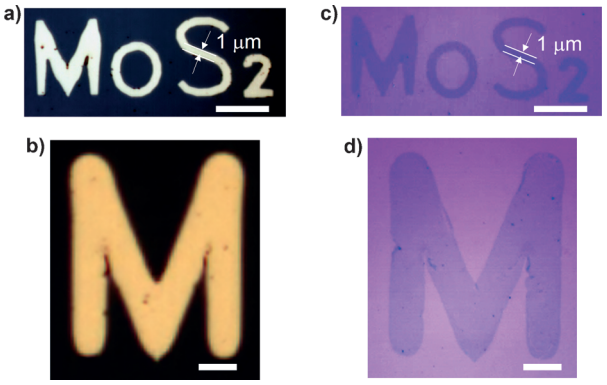

Figure 4. a), b) Optical microscope images of Au patterns on Si substrates obtained by electron-beam lithography. c), d) Patterned MoS_2 atomic layers corresponding to (a) and (b), respectively. Note that (c) and (d) are taken after transferring MoS_2 atomic layers formed on (a) and (b) onto new SiO_2 substrates. All of the scale bars are 10 μm.

with H_2S completes the formation of MoS_2 atomic layers. By simply defining the pattern of Au film, patterned growth of MoS_2 atomic layers has been also achieved. Our method illuminates a simple inspection for the utilization of bimetal surface alloy (Mo-Au) that successfully provides an ideal environment maximizing the reactivity between Mo and S on a solid substrate. We believe that other proper sets of catalytic substrate and metal precursor would prepare various TMDs in atomic layers not only in large-scale but also in desired patterns with high uniformity.

Experimental Section

Synthesis of atomic layers of MoS_2 on Au film (Supporting Information, Figure S2a): A 50 nm thick Au film was deposited on a pre-cleaned Si(100) substrate by electron-beam evaporation. The substrate was located in a protection quartz tube that is placed at the center of electric tube furnace. Molybdenum hexacarbonyl ($[Mo(CO)_6]$; 0.1 g, Aldrich, 99%) was loaded on a ceramic boat and placed at the upstream verge slightly outside of the furnace. Ar gas was then supplied at 300 sccm for 10 min to purge the quartz tube then heated by closing the top lid of the furnace up to 300 °C at the rate of 30 °C per minute, under which the temperature applied to $[Mo(CO)_6]$ becomes about 66 °C. After 30 min, 5 sccm of H_2S gas was supplied for another 30 min for sulfidation reaction. After the reaction was completed, the furnace was cooled down at the rate of 50 °C per minute by opening the top lid of the furnace under Ar atmosphere.

Received: October 31, 2013
Published online: January 13, 2014

Keywords: 2D nanomaterials · chemical vapor deposition · molybdenum disulfide · patterned growth · surface alloys

[1] K. Mak, C. Lee, J. Hone, J. Shan, T. Heinz, *Phys. Rev. Lett.* **2010**, *105*, 2 – 5.
[2] B. Radisavljevic, A. Radenovic, J. Brivio, V. Giacometti, A. Kis, *Nat. Nanotechnol.* **2011**, *6*, 147 – 150.
[3] Q. H. Wang, K. Kalantar-Zadeh, A. Kis, J. N. Coleman, M. S. Strano, *Nat. Nanotechnol.* **2012**, *7*, 699 – 712.
[4] H. Zeng, J. Dai, W. Yao, D. Xiao, X. Cui, *Nat. Nanotechnol.* **2012**, *7*, 490 – 493.
[5] K. F. Mak, K. He, J. Shan, T. F. Heinz, *Nat. Nanotechnol.* **2012**, *7*, 494 – 498.
[6] L. Britnell, R. V. Gorbachev, R. Jalil, B. D. Belle, F. Schedin, A. Mishchenko, T. Georgiou, M. I. Katsnelson, L. Eaves, S. V. Morozov, et al., *Science* **2012**, *335*, 947 – 950.
[7] M. P. Levendorf, C.-J. Kim, L. Brown, P. Y. Huang, R. W. Havener, D. A. Muller, J. Park, *Nature* **2012**, *488*, 627 – 632.
[8] Y.-H. Lee, X.-Q. Zhang, W. Zhang, M.-T. Chang, C.-T. Lin, K.-D. Chang, Y.-C. Yu, J. T.-W. Wang, C.-S. Chang, L.-J. Li, et al., *Adv. Mater.* **2012**, *24*, 2320 – 2325.
[9] X. Wang, H. Feng, Y. Wu, L. Jiao, *J. Am. Chem. Soc.* **2013**, *135*, 5304 – 5307.
[10] Y.-C. Lin, W. Zhang, J.-K. Huang, K.-K. Liu, Y.-H. Lee, C.-T. Liang, C.-W. Chu, L.-J. Li, *Nanoscale* **2012**, *4*, 6637 – 6641.
[11] Y. Zhan, Z. Liu, S. Najmaei, P. M. Ajayan, J. Lou, *Small* **2012**, *8*, 966 – 971.
[12] K.-K. Liu, W. Zhang, Y.-H. Lee, Y.-C. Lin, M.-T. Chang, C.-Y. Su, C.-S. Chang, H. Li, Y. Shi, H. Zhang, et al., *Nano Lett.* **2012**, *12*, 1538 – 1544.
[13] M. Schleberger, D. Fujita, C. Scharfschwerdt, S. Tougaard, *Surf. Sci.* **1995**, *331 – 333*, 942 – 947.
[14] T. Massalski, H. Okamoto, *J. Phase Equilib.* **1986**, *7*, 449 – 452.
[15] R. Chellappa, D. Chandra, *J. Chem. Thermodyn.* **2005**, *37*, 377 – 387.
[16] C. Lee, H. Yan, L. E. Brus, T. F. Heinz, J. Hone, S. Ryu, *ACS Nano* **2010**, *4*, 2695 – 2700.
[17] Z. Zeng, Z. Yin, X. Huang, H. Li, Q. He, G. Lu, F. Boey, H. Zhang, *Angew. Chem.* **2011**, *123*, 11289 – 11293; *Angew. Chem. Int. Ed.* **2011**, *50*, 11093 – 11097.
[18] J. N. Coleman, M. Lotya, A. O'Neill, S. D. Bergin, P. J. King, U. Khan, K. Young, A. Gaucher, S. De, R. J. Smith, et al., *Science* **2011**, *331*, 568 – 571.
[19] J. Brivio, D. T. L. Alexander, A. Kis, *Nano Lett.* **2011**, *11*, 5148 – 5153.
[20] Y. Feldman, E. Wasserman, D. J. Srolovitz, R. Tenne, *Science* **1995**, *267*, 222 – 225.
[21] Y. Feldman, G. L. Frey, M. Homyonfer, V. Lyakhovitskaya, L. Margulis, H. Cohen, G. Hodes, J. L. Hutchison, R. Tenne, *J. Am. Chem. Soc.* **1996**, *118*, 5362 – 5367.
[22] J. Tersoff, *Phys. Rev. Lett.* **1995**, *74*, 434 – 437.
[23] C. Stampfl, M. Scheffler, H. Over, J. Burchhardt, M. Nielsen, D. Adams, W. Moritz, *Phys. Rev. Lett.* **1992**, *69*, 1532 – 1535.
[24] P. L. Nielsen, F. Besenbacher, I. Stensgaard, E. Laegsgaard, C. Engdahl, P. Stoltze, K. Jacobsen, J. Norskov, *Phys. Rev. Lett.* **1993**, *71*, 754 – 757.
[25] X. L. Li, G. Ouyang, G. W. Yang, *Nanotechnology* **2008**, *19*, 505303.
[26] J. Rodriguez, M. Kuhn, *Surf. Sci.* **1995**, *330*, L657 – L664.
[27] P. Liu, J. A. Rodriguez, J. T. Muckerman, J. Hrbek, *Surf. Sci.* **2003**, *530*, L313 – L321.
[28] C. Gelatt, H. Ehrenreich, *Phys. Rev. B* **1974**, *10*, 398 – 415.
[29] F. Gao, D. W. Goodman, *Chem. Soc. Rev.* **2012**, *41*, 8009 – 8020.
[30] M. M. Biener, J. Biener, R. Schalek, C. M. Friend, *Surf. Sci.* **2005**, *594*, 221 – 230.
[31] Z. Song, T. Cai, J. A. Rodriguez, J. Hrbek, A. S. Y. Chan, C. M. Friend, *J. Phys. Chem. B* **2003**, *107*, 1036 – 1043.
[32] S. Helveg, J. Lauritsen, E. Laegsgaard, I. Stensgaard, J. Norskov, B. Clausen, H. Topsoe, F. Besenbacher, *Phys. Rev. Lett.* **2000**, *84*, 951 – 954.
[33] M. M. Biener, J. Biener, R. Schalek, C. M. Friend, *J. Chem. Phys.* **2004**, *121*, 12010 – 12016.
[34] M. M. Biener, C. M. Friend, *Surf. Sci.* **2004**, *559*, L173 – L179.

